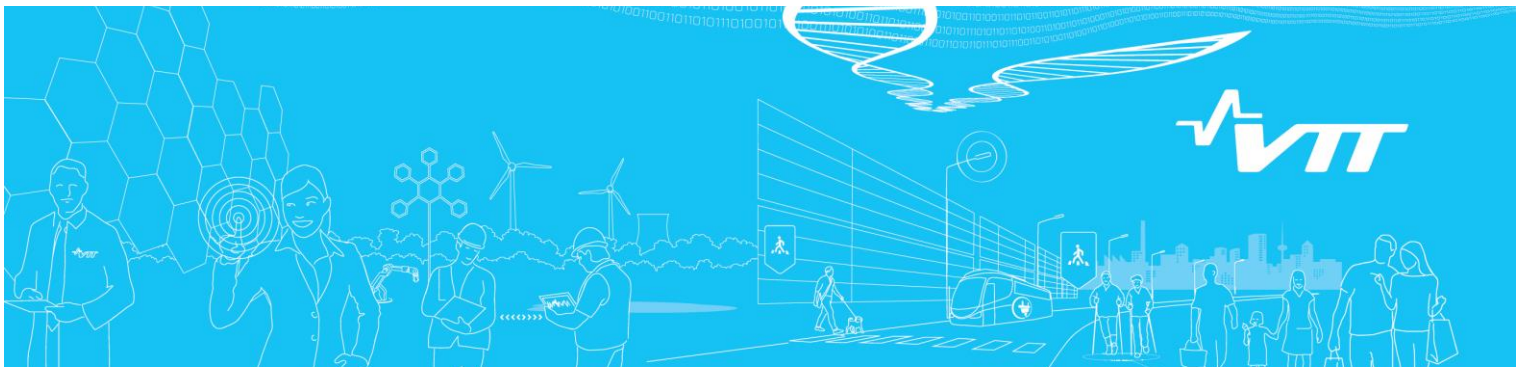

RESEARCH REPORT

VTT-R-00953-18

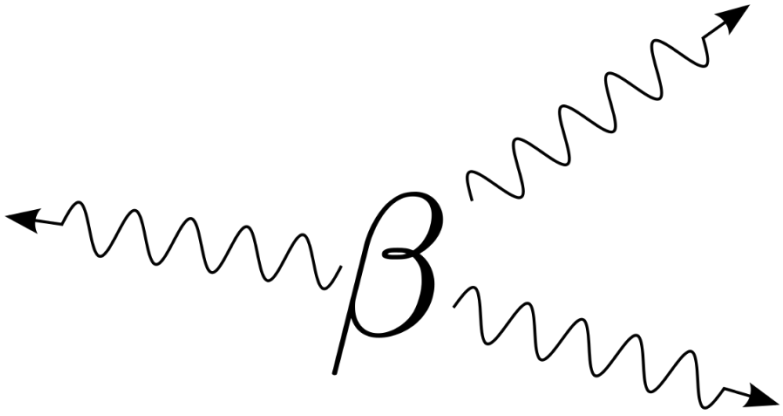

Implementing a beta bremsstrahlung source in Serpent

Authors: Toni Kaltiaisenaho

Confidentiality: Public

Report's title	
Implementing a beta bremsstrahlung source in Serpent	
Customer, contact person, address	**Order reference**
Project name	**Project number/Short name**
KATVE 2017/SAFIR2018	113443
Author(s)	**Pages**
Toni Kaltiaisenaho	24
Keywords	**Report identification code**
Serpent, Monte Carlo, beta decay, bremsstrahlung	VTT-R-00953-18

Summary

In this report, a beta bremsstrahlung model implemented in Serpent Monte Carlo code is described. The beta spectrum model includes a theoretical shape factor for beta transitions. The transition types, energies and intensities are read from an ENDF format decay data file. A simple approximation for the Fermi function is used. Bremsstrahlung photons emitted by beta particles are created with a thick-target bremsstrahlung approximation.

The implemented beta bremsstrahlung model is compared to Geant4 Monte Carlo code in a simple fuel pin geometry for Sr-90 and Y-90. A reasonably good agreement is obtained in the peak regions of the bremsstrahlung spectra. Serpent underestimates the spectra in the high-energy regions, which is most likely due to the limitations of the thick-target bremsstrahlung approximation. The beta spectrum model is also compared to RADAR beta spectrum data for a few nuclides by calculating effective dose rate around a fuel pin. The dose rates calculated with the Serpent beta spectrum model are a few percent higher on average.

Confidentiality	Public

Espoo 3.4.2018

Written by	Reviewed by	Accepted by
Toni Kaltiaisenaho, Research Scientist	Jaakko Leppänen, Research Professor	Petri Kotiluoto, Research Team Leader

VTT's contact address

Distribution (customer and VTT)

Contents

1 Introduction

Beta decay calculations are needed in many applications, for example in estimating decay heat from spent nuclear fuel [1], radiotherapy and dosimetry [2, 3], studying nuclear batteries [4] and in radiation protection [5]. In shielding applications, it is important to take into account bremsstrahlung emitted by beta particles as they slow down in matter. Bremsstrahlung production is important for high-energy beta particles, especially in heavy materials like nuclear fuel. Bremsstrahlung emitted by beta particles can contribute 10–20% to the total photon dose rate in spent fuel [6].

The Serpent Monte Carlo code [7] includes a radioactive decay source mode, which can be used e.g. for shielding calculations involving spent fuel. The decay source mode can be conveniently used with the built-in burnup calculation mode. In this work, the decay source mode is expanded to include bremsstrahlung from beta particles and internal conversion electrons. Beta spectrum is calculated using a theoretical model which utilizes ENDF format beta transition data. In addition, support for user-defined beta spectrum data is included. Bremsstrahlung photons are created using a thick-target bremsstrahlung approximation, which was originally implemented as a part of the photon transport mode [8].

A theoretical description of the implemented beta decay model is given first, and available beta spectrum data and codes are discussed. Details of the implementation are then described. The beta bremsstrahlung model is compared to Geant4 Monte Carlo code [9] and to RADAR beta spectrum data [10] for a few nuclides.

2 Beta decay theory and data

To simulate a beta decay emission with the Monte Carlo method, the spectrum of emitted betas is required, which is used for sampling the initial energy of the particles. The spectrum can either be calculated by the Monte Carlo code using some theoretical model, or it can be given as an input data to the code. Here, a simple theoretical model of beta spectrum is presented first, after which a brief overview of available beta spectrum data and codes is given.

2.1 Spectrum of beta decay

In beta decay, a parent nucleus X with an atomic number Z and mass number A decays into a daughter nucleus Y by emitting two leptons: a beta particle and neutrino. The mass number of the nucleus remains unchanged while the atomic number changes by ± 1. In beta minus (β^-) decay, an electron and antineutrino are emitted and the daughter nucleus has an atomic number $Z+1$, which is written as

$$ {}^{A}_{Z}X \rightarrow {}^{A}_{Z+1}Y + e^- + \overline{\nu}_e. \tag{2.1} $$

In beta plus (β^+) decay, a positron and neutrino are emitted and the daughter nucleus has an atomic number $Z-1$:

$$ {}^{A}_{Z}X \rightarrow {}^{A}_{Z-1}Y + e^+ + \nu_e. \tag{2.2} $$

The transition energy for β^- decay is given by[1]

$$ T_i = \left[M(Z,A) - M(Z+1,A)\right] c^2 - E_l, \tag{2.3} $$

where $M(Z,A)$ and $M(Z+1,A)$ are the atomic masses of the ground states of the parent and daughter, respectively, E_l is the energy level to which the decay occurs and i indicates the transition. For β^+ decay, the transition energy is given by

$$ T_i = \left[M(Z,A) - M(Z-1,A)\right] c^2 - 2m_\mathrm{e}c^2 - E_l. \tag{2.4} $$

where m_e is the rest mass of electron. Eq. (2.4) sets an energy limit above which β^+ decay can occur:

$$ \left[M(Z,A) - M(Z-1,A)\right] c^2 - E_l > 2m_\mathrm{e}c^2. \tag{2.5} $$

A process competing with β^+ decay is electron capture which can occur below this energy limit.

The transition energy is shared between the beta particle and neutrino[2]. The energy spectrum of beta decay can be written as [12]

$$ N(E)dE \propto C(E)F(Z,E)pE(E_i - E)^2 dE, \tag{2.6} $$

[1] Changes in electron binding energies are ignored here.

[2] The recoil energy of the daughter nucleus is usually of the order of 10 to 100 eV [11] which is negligible in comparison to the transition energy.

Table 2.1: Classification of beta transitions according to the change in total angular momentum ΔJ and parity $\Delta\pi$.

Transition type	$\lvert\Delta J\rvert$	$\Delta\pi$
Super-allowed	0	$+1$
Allowed	$0, 1$	$+1$
1st forbidden unique	2	-1
2nd forbidden unique	3	$+1$
nth forbidden unique	$n+1$	$(-1)^n$
1st forbidden non-unique	$0, 1$	-1
2nd forbidden non-unique	2	$+1$
nth forbidden non-unique	n	$(-1)^n$

where E is the total energy and p is the momentum of the beta particle, $E_i = T_i + m_e c^2$ is the maximum total energy of the beta particle, $C(E)$ is the shape factor, $F(Z, E)$ is the Fermi function and Z is the atomic number of the daughter nucleus. The role of the Fermi function $F(Z, E)$ is to take into account the effect of the Coulomb field of the daughter nucleus on the emitted beta particle, whereas the shape factor introduces energy-dependent effects caused by the coupling between the nuclear structure and lepton dynamics. Other multiplicative factors can also be introduced in Eq. (2.6), which take into account atomic screening effects, radiative corrections and finite nuclear charge [12, 13].

The shape factor depends on the transition type which is determined by the change in total angular momentum (ΔJ) and change in the parity ($\Delta\pi$) between the parent and daughter nucleus. The transition types are listed in Table 2.1. The shape factor for allowed and forbidden unique transitions is given by [12]

$$C(E) = (2L-1)! \sum_{k=1}^{L} \lambda_k \frac{p^{2(k-1)} q^{2(L-k)}}{(2k-1)!\,[2(L-k)+1]!}, \tag{2.7}$$

where $L = 1$ for an allowed or super-allowed transition and $L = n + 1$ for nth forbidden unique transition. The parameter λ_k is defined by the Coulomb amplitudes of the electron wave functions, and its calculation is not straightforward. The usual approximation is to set $\lambda_k = 1$, which is also assumed in this work. With this assumption, the shape factor for an allowed transition becomes $C(E) = 1$. According to Ref. [12], calculation of beta spectrum for non-unique transitions is a lot more complicated than for unique transitions. As an approximation, non-unique transitions are often treated as unique transitions with the same $|\Delta J|$, from which follows that $L = n$ in Eq.(2.7) for an nth forbidden non-unique transition. Shape factors have also been determined experimentally for some nuclides. A compilation of experimental shape factors for allowed, forbidden unique and non-unique transitions is given in Ref. [12].

The Fermi function for a point-like nuclear charge calculated from the Dirac equation

is given by [14]

$$F(Z,E) = 2(1+\gamma_0)(2pR/\hbar)^{-2(1-\gamma_0)} e^{\pi\nu} \frac{|\Gamma(\gamma_0 + i\nu)|^2}{[\Gamma(2\gamma_0+1)]^2}, \tag{2.8}$$

where Γ is the gamma function, R is the nuclear radius, and γ_0 and ν are defined as

$$\gamma_0 = \sqrt{1-(\alpha Z)^2}, \tag{2.9}$$

$$\nu = \pm\frac{\alpha Z E}{pc}, \tag{2.10}$$

where α is the fine-structure constant and $+$ $(-)$ corresponds to an electron (positron). Multiple tabulations and approximations for the Fermi function have been given in the literature (see e.g. Ref. [15, 16] and the references therein). We use the simple approximation derived by Venkataramaiah et al. [16], which for electrons is given by

$$F(Z,E) = \sqrt{A + \frac{B}{E/m_e c^2 - 1}}, \tag{2.11}$$

where

$$A = \begin{cases} mZ + K & \text{if } Z < 16 \\ 1 + a_0 \exp(b_0 Z) & \text{if } Z \geq 16 \end{cases}, \tag{2.12}$$

$$B = aZ\exp(bZ)\,. \tag{2.13}$$

The constants m, K, a_0, b_0, a and b are defined as

$$m = 7.30\times10^{-2} \qquad K = 9.40\times10^{-1}, \tag{2.14}$$

$$a_0 = 404.56\times10^{-3} \qquad b_0 = 73.184\times10^{-3}, \tag{2.15}$$

$$a = \begin{cases} 5.5465\times10^{-3} & \text{if } Z \leq 56 \\ 1.2277\times10^{-3} & \text{if } Z > 56 \end{cases}, \tag{2.16}$$

$$b = \begin{cases} 76.929\times10^{-3} & \text{if } Z \leq 56 \\ 101.22\times10^{-3} & \text{if } Z > 56 \end{cases}. \tag{2.17}$$

According to Venkataramaiah et al., this approximation reproduces the tabulated values given in Ref. [17] within an error of one percent.

To use the Fermi function approximation (2.11) for positrons, it must by multiplied by the ratio of the positron Fermi function $F_+(Z,e)$ and electron Fermi function $F_-(Z,e)$, which is given by

$$\frac{F_+(Z,e)}{F_-(Z,e)} = e^{-2\pi|\nu|}\frac{|\Gamma(\gamma_0 - i|\nu|)|^2}{|\Gamma(\gamma_0 + i|\nu|)|^2} = e^{-2\pi|\nu|}, \tag{2.18}$$

where the property $\overline{\Gamma(z)} = \Gamma(\overline{z})$ has been used.

2.2 Overview of beta decay codes and spectrum data

Serpent reads and processes ENDF format decay data which is used e.g. in ENDF/B-VII.1 [18], JEFF-3.1.1 [19], JEFF-3.3 [20] and JENDL/DDF-2015 [21] decay libraries. The ENDF format decay data supports both discrete and continuous beta spectra. Discrete beta spectrum data refers to beta transitions, and the data includes the energies, relative intensities and types of transitions. According to the ENDF-6 Formats Manual [22], allowed, 1st forbidden unique and 2nd forbidden unique transitions are specified separately, but non-unique transitions are classified as allowed transitions (they share the same TYPE value in the data). The ENDF-6 format data also contains the intensities and energies for internal conversion and Auger electrons which are classified as "discrete electrons" in the ENDF-6 Formats manual. The average decay energies for all types of emissions are also given.

The ENDF/B-VII.1 decay library contains continuous β^- spectrum data for 280 nuclides[3]. These 280 nuclides also have continuous gamma spectra and 230 of them have continuous neutron spectra, which means that most of them are beta-delayed neutron emitters. Discrete beta spectrum is given for 733 β^--emitters and 498 β^+-emitters[4].

In both JEFF-3.1.1 and JEFF-3.3, continuous β^- spectra is given only for 33 nuclides of which 32 also have continuous neutron spectra. Both libraries have discrete β^- spectra for 672 nuclides, and discrete β^+ spectra is given for 409 and 422 nuclides in JEFF-3.1.1 and JEFF-3.3, respectively. In both libraries, the transition type is not always specified (parameter TYPE=0.0). Some transitions have TYPE=4.0 which probably stands for a 3rd forbidden unique transition, although this TYPE value is not defined in the ENDF-6 Formats Manual [22].

The JENDL/DDF-2015 decay library, which contains the fission product nuclide data from JENDL/FPD-2011 [23], includes discrete and continuous β^- spectra for 842 and 486 nuclides, respectively. Discrete β^+ spectra is given for 781 nuclides. The continuous β^- spectra belong to fission product nuclides, and they have been theoretically estimated due to the short half-lives of the nuclides and lack of measured data. Some of the nuclides that have continuous beta spectrum data also have discrete beta transition data. Some problems with the JENDL/DDF-2015 data were detected. Multiple β^+/EC transitions, for which positron emission is not energetically possible, have non-zero positron intensities. In some cases, the transition energy or the discrete spectrum normalization factor is zero. The β^+ transition energies of the nuclides Y-78 and Y-78m are above 10 GeV, which are obviously incorrect.

A reasonably extensive compilation of beta decay spectrum data can be found on the RAdiation Dose Assessment Resource (RADAR) website [10,24], which contains beta spectra for about 460 nuclides. The data is given in an excel sheet which has somewhat incoherent structure. For example, isomeric states are poorly labelled and the type of decay is unclear in some cases. Also, the spectrum values at zero

[3]The numbers of beta-decaying nuclides given here were calculated in the decay data processing routines in Serpent.

[4]Note that some nuclides can have both beta decay modes, such as Cu-64.

and at maximum beta energy are not given for most nuclides, which means that the data must be extrapolated by the user. For most nuclides, the RADAR data is from Ref. [25], and for some nuclides the RadList code [26] is cited.

ICRP Publication 107 includes beta spectrum data for about thousand nuclides [27]. The data can be downloaded from Ref. [28]. Unfortunately, this data source was discovered when this report was almost finished, and thus was not used in this report.

A handful of codes have been developed for calculating beta spectrum. These include RadList [26] (also known as RADLIST and RADLST), BTSPEC [29], BETASP [30] and BetaShape [12, 13]. BTSPEC and BETASP are available through NEA Data Bank [31, 32], whereas RadList and BetaShape are listed as ENSDF analysis and utility programs [33]. The RadList program (including the source code) can be downloaded from the ENSDF website, whereas BetaShape is available (executable only) from the Laboratoire National Henri Becquerel (LNHB) website [34].

All the codes listed above have been developed in the '70s or '80s, with the exception of BetaShape which was released in 2016. Of these codes, RadList is probably most commonly used for calculating beta spectrum. BTSPEC is used by the JANIS [35] nuclear data information program for plotting beta spectrum. BetaShape is used as a reference code for the Decay Data Evaluation Project (DDEP) evaluations [20]. At least RadList and BetaShape use ENSDF nuclear decay data for calculating beta spectra.

3 Implementation in Serpent

The radioactive decay source was introduced in Serpent 2.1.24 which initially handled only discrete photon spectra. Support for neutron emission and continuous spectra were added in version 2.1.29. The decay source mode can be used in succession to a burnup calculation, which provides a restart file containing radioactive material compositions. It is also possible for the user to define radioactive material compositions in the input file. Decay constants and emission spectra needed for a decay calculation are read from an ENDF format decay data file.

In Serpent, decay emissions are treated independently of each other, which means that individual decays are not simulated. There are two modes for sampling the decay location in the geometry. In the analog mode, a decay location is first sampled uniformly throughout the geometry, and the location is accepted based on the ratio of the location's material emission rate[5] to the maximum material emission rate of the simulated particle type. In the implicit mode, the location is uniformly sampled, and the weight of the emitted particle is adjusted by the ratio of the location's material emission rate to the average emission rate. It is also possible to define only a single radioactive material, in which case there is no difference between the analog and implicit sampling modes.

[5] In the units of emitted particles per second per material volume.

To obtain physical results from a Monte Carlo simulation, the calculated quantities must be normalized correctly. In the case of a single particle type decay calculation (a photon or neutron source), the normalization coefficient is calculated in Serpent as the ratio of the particle type's total decay source rate to the particle type's total sampled source rate. When both photons and neutrons are used, normalization is done with respect to the neutron source, which also requires the adjustment of the particle weight by the ratio of the particle type's decay source rate to the neutron's decay source rate. This normalization method is somewhat impractical when the decay source consists of more than two particle types. Therefore, a more generalized approach was added in Serpent. The normalization coefficient is calculated as the ratio of the total decay source rate of all the particle types included in the simulation to their total sampled source rate. This requires no adjustment of the particle weight in the decay source routine. Total material emission rates (summed over the simulated particle types) are used in the sampling of the decay location with the analog or implicit mode described above. Once the decay location has been sampled, the particle type is chosen with a probability given by the decay source rate of the type in the location's material. This approach means that the number of source particles used in a decay calculation refers to all the particle types included in the simulation instead of a single type. A support for this "multiparticle" source was added in the source definition. Defining a multiparticle source for a decay calculation works simply by including the particle types in the source card. New particle types were added to enable beta decay simulation. Using "electron" or "e" in the source definition enables β^- decay, "positron" or "pos" enables β^+ decay and "beta" or "b" enables both.

To enable the simulation of beta decay and discrete electron emissions, Serpent processing routines were modified to read the relevant data from an ENDF format decay file. Continuous beta and discrete electron spectra didn't require any major modifications in the routines. In the case of discrete beta transitions, energies, relative intensities and types of transitions are read and processed. For β^+ transitions, $2m_\mathrm{e}c^2$ is subtracted from the transition energy, and the transition is included only if the resulting energy is positive. The intensity of a β^+ transition is given by the RIS parameter instead of the usual RI parameter [22]. If the type of the transition is not specified (parameter TYPE=0.0 in the ENDF decay data), it is assumed to be an allowed transition. If the parameter TYPE has a higher value than 3.0, it is assumed to be a (TYPE-1)th forbidden unique transition.

If discrete beta transitions are given for a nuclide, the spectrum for each transition is calculated using the theoretical model described in Sec. 2.1. The total beta spectrum for the nuclide is calculated as

$$N_\mathrm{tot}(T)dT \propto \sum_i I_i \frac{C(E)F(Z,E)pE(T_i - T)^2}{\int_0^{T_i} C(E')F(Z,E')p'E'(T_i - T')^2 dT'} dT, \tag{3.1}$$

where T is the kinetic energy of the beta particle and I_i is the relative intensity of the beta transition. This spectrum is normalized to unity to form a probability density function (PDF) and cumulative distribution function (CDF). Linear interpolation is used in the integration. The total relative intensity of the beta emission is given by the sum of the transition intensities. The energy grid, at which the transition and

total spectra are evaluated, consists of all the transition energies with an addition of 150 equidistant points between 1 eV and the highest transition energy and 10 equidistant points between 1 eV and the lowest transition energy.

An option for replacing the Serpent-calculated beta spectra with user-given data was also added. It is possible to replace beta spectrum for a single or multiple nuclides. User-defined spectra can be used only for those nuclides for which beta transitions are given in the ENDF decay data. Replacing continuous ENDF beta spectra was not implemented.

In the decay source routine, the energy of a beta particle or discrete electron is sampled using already implemented routines. Thick-target bremsstrahlung approximation (TTB) is used for sampling the number and energies of bremsstrahlung photons emitted by betas. The photons are emitted on the decay location, neglecting the transport of betas in the matter. The TTB approximation implemented in Serpent is based on the continuous slowing down approximation (CSDA), which assumes that electrons lose their energy in a continuous manner. This assumption is not valid when energy loss through bremsstrahlung is important (above a few MeV or so in materials composed of heavy elements), because a high-energy electron or positron can lose a large quantity of energy in a single bremsstrahlung interaction. This results in the underestimation of bremsstrahlung yield by the CSDA, and subsequently by the TTB approximation.

It is important to note that positron annihilation is not simulated in Serpent after β^+ decay because ENDF format decay data already contains the contribution from the two annihilation photons. If electron transport is implemented in Serpent in the future, this emission component should be removed during the processing of the decay data.

4 Test cases

Three test cases were constructed for validating the implemented beta decay model: a normalization test case, a comparison to Geant4 and a comparison to the RADAR beta spectrum data. The beta bremsstrahlung model was used with the development version of Serpent 2.1.30. The ENDF/B-VII.1 decay library was used in all Serpent calculations presented here.

4.1 Normalization test case

This test case was performed in order to verify that the modified decay source routine simulates the emission of all particle types properly, and that the normalization of the results is correct. A very small cylinder composed of two radioactive and one non-active material regions was used as a test geometry. Two nuclides, Cs-143 and Rb-96, both of which emit neutrons, gammas and betas, were used. Photon and neutron spectra were calculated on the outer surface of the geometry with Serpent 2.1.29 and the development version which included the beta bremsstrahlung

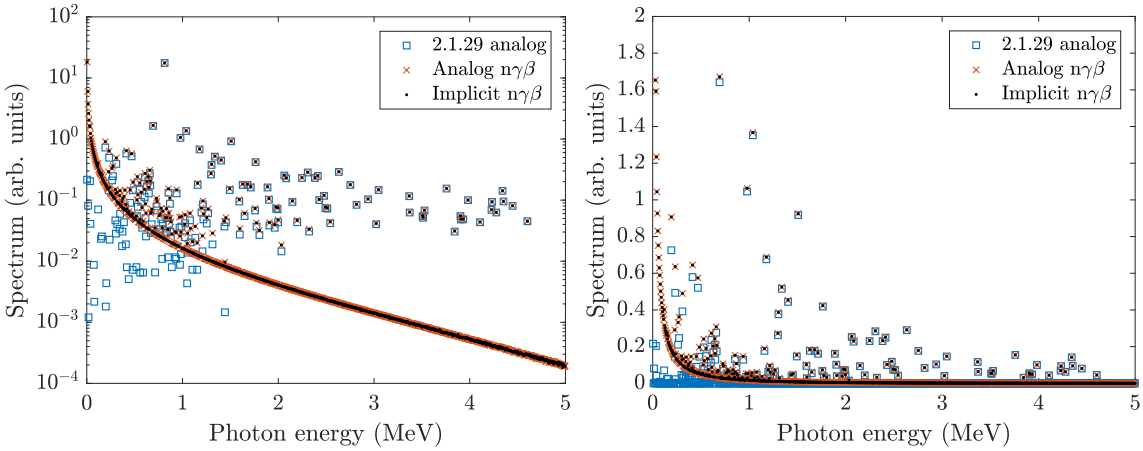

Figure 4.1: Photon spectrum in the normalization test case calculated with Serpent 2.1.29 using the analog sampling mode, and with the n$\gamma\beta$-source using both the analog and implicit sampling modes. The whole tallied spectrum is shown on the left and a close-up of the low-intensity peaks is shown on the right.

model. Neutron, photon and beta emissions were simulated using a single source (here referred to as n$\gamma\beta$-source) with the development version, whereas neutron and photon transport simulations were run separately with Serpent 2.1.29. Both the analog and implicit decay sampling modes were tested. The photon spectrum calculated with the development version was also compared to a semi-analytical photon emission spectrum.

The used geometry consists of three joined cylinders, each with a radius of 10^{-8} cm. The first cylinder is composed of Cs-143 and has a height of 3×10^{-8} cm, the second one is composed of natural iron and has a height of 10^{-8} cm and the third one is made of Rb-96 and has a height of 10^{-8} cm. The two cylinders containing Cs-143 and Rb-96 have different sizes in order to detect any size-dependent discrepancies between the analog and implicit decay sampling modes. The natural iron, which consists of stable isotopes, is included to find any material-dependent problems in the sampling modes.

Cs-143 has two decay modes, the first one is a β^- decay into Ba-143 with a branching ratio of 98.36%, and the second one is a β^- decay followed by a neutron emission into Ba-142 with a branching ratio of 1.64%. Rb-96 has a β^- decay mode with a branching ratio of 86.7% and a β^- decay followed by a neutron emission mode with a branching ratio of 13.3%. Both nuclides have a complex discrete gamma spectrum and they emit high-energy betas; the average energy of beta radiation is 2.39 MeV for Cs-143 and 3.94 MeV for Rb-96. The half-lives of Cs-143 and Rb-96 are about 1.8 s and 0.2 s, respectively.

Due to the small size of the cylinder, practically all the emitted particles escape the geometry without interacting with the cylinder materials. Therefore, the spectrum calculated on the outer surface of the geometry should be equal to the total decay emission spectrum. This can be used to verify that the normalization of the results is done correctly. For this test case, photon emission spectrum was calculated semi-analytically from the emission spectra of gammas and betas. The discrete gamma

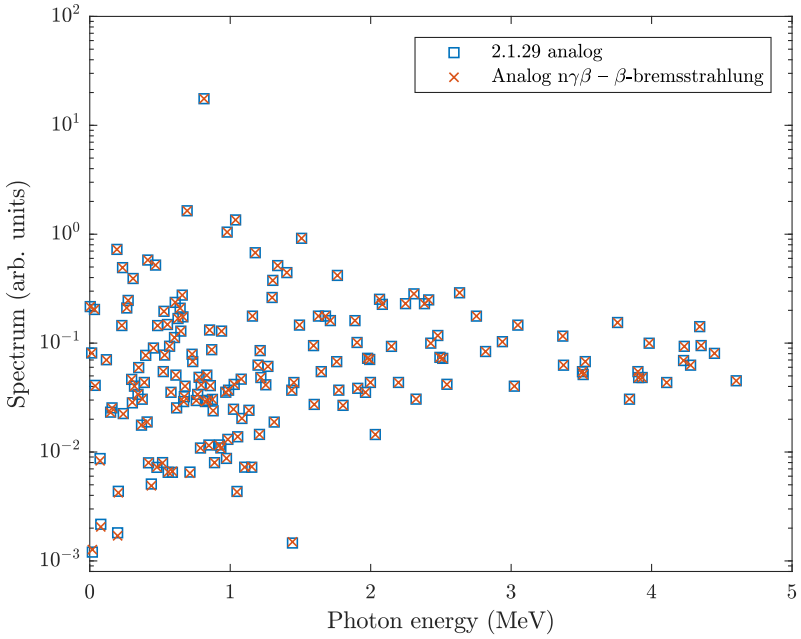

Figure 4.2: Gamma peaks in the normalization test case. The squares correspond to the peaks calculated with Serpent 2.1.29, whereas the crosses correspond to the peaks calculated with the nγβ-source from which the beta bremsstrahlung component has been subtracted.

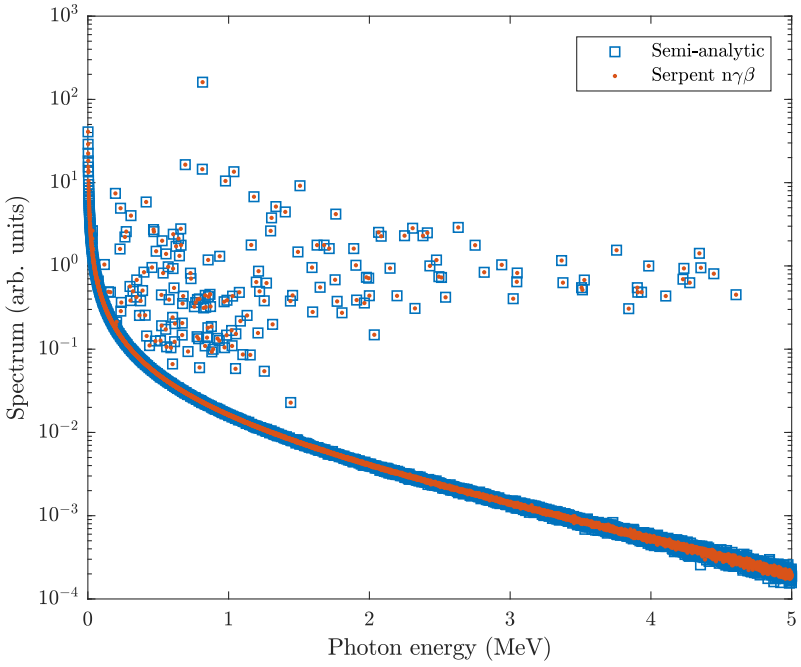

Figure 4.3: Photon spectrum in the normalization test case calculated semi-analytically and with the nγβ-source.

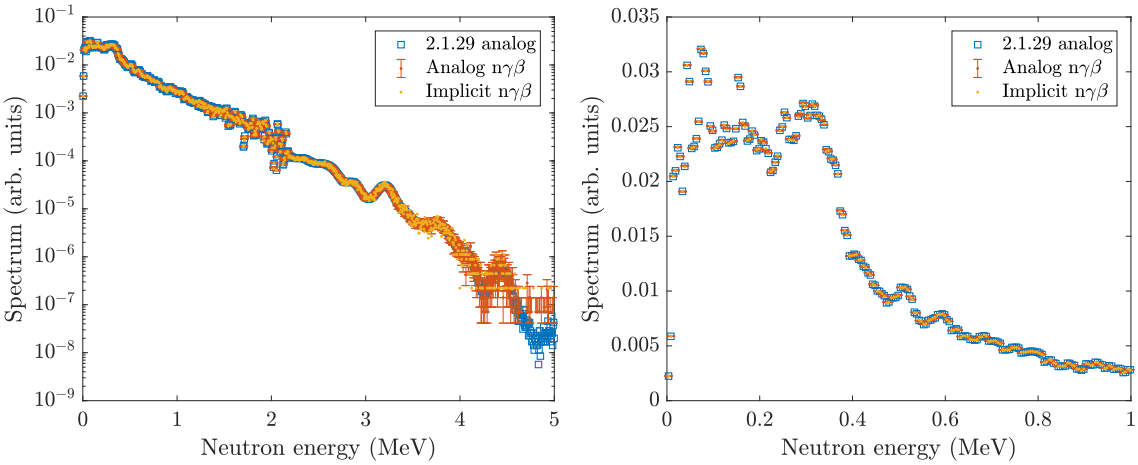

Figure 4.4: Neutron spectrum in the normalization test case calculated with Serpent 2.1.29 using the analog sampling mode, and with the n$\gamma\beta$-source using both the analog and implicit sampling modes. The whole tallied spectrum is shown on the left and a close-up between 0 and 1 MeV is shown on the right.

energies were simply included by multiplying the relative intensity of each energy by the activity of the material. The beta bremsstrahlung component was calculated with a Monte Carlo simulation, i.e. in the same way as is done in the decay source routine in Serpent.

The calculated photon spectra are plotted in Fig. 4.1. There is an excellent match between the spectra obtained with the analog and implicit sampling mode. The intensities of the gamma peaks obtained with Serpent 2.1.29 are very close to the ones calculated with the n$\gamma\beta$-source in the region where bremsstrahlung intensity is low, above 1.5 MeV or so. Below this energy the effect of beta bremsstrahlung is clearly visible with the n$\gamma\beta$-source. Fig. 4.2 shows the photon spectrum calculated with the n$\gamma\beta$-source from which the separately calculated bremsstrahlung component has been subtracted. The agreement with Serpent 2.1.29 is excellent. The semi-analytic spectrum is plotted in Fig. 4.3 together with the photon spectrum calculated with the n$\gamma\beta$-source, showing great agreement. The neutron spectrum plotted in Fig. 4.4 also shows excellent agreement. Based on these results, the implemented n$\gamma\beta$-source works correctly for photons and neutrons in both sampling modes.

4.2 Comparison to Geant4

In this test case, the beta bremsstrahlung model implemented in Serpent is compared to Geant4 Monte Carlo code [9] which is a general-purpose toolkit for simulating particle transport through matter. Geant4 includes a radioactive decay module (RDM), which is a package used for simulating radioactive decays [36]. Geant4 has two approaches for simulating radioactive decay. The first one is per-decay sampling in which individual decay events are simulated one by one. The second one is statistical sampling in which all decay emissions are treated independently from each other. Geant4 does not include a built-in class for simulating radioactive materials, and only single radioactive nuclides can be simulated with the built-in

commands. According to Ref. [36] from 2013, Geant4 has used the same Fermi function approximation as Serpent, but an inspection of the source code showed that a more complex beta decay model has been implemented since.

A single fuel pin consisting of UO2 with a minute concentration of Sr-90 or Y-90 was used as a test geometry. A fuel pin can be regarded as a typical smallest geometrical component in spent fuel calculations for which the Serpent beta bremsstrahlung model is intended to be used. Therefore, it is important to study the validity of the beta decay model and the TTB approximation in this geometry. Sr-90 and Y-90 were selected as they are important β^- emitters among medium-lived fission products, especially Y-90. Sr-90 decays into Y-90 with a half-life of 28.8 years. It is a pure β^- emitter with a maximum and average β^- energies of 546 keV and 196 keV, respectively. Y-90 can be considered as a pure β^- emitter, because the $\beta^-_{0,0}$ transition dominates with a relative intensity of 0.9998 per decay. The maximum and average energies of this transition are 2279 keV and 927 keV, respectively. The half-life of Y-90 is 2.67 days.

In the geometry, the radius and height of the fuel pin are 0.4025 cm and 100 cm, respectively. The fuel is surrounded by cladding with a thickness of 0.075 cm, and the pin is surrounded by an air cylinder with a radius of 1 cm. The mass fraction of Sr-90 or Y-90 is 1×10^{-6} in the fuel. In the Serpent calculations, photon spectrum was tallied on the surface of the air cylinder surrounding the fuel pin. In the Geant4 simulations, photons and electrons crossing the surface of the air cylinder were printed to an output file. Geant4 spectra were generated in the post-processing phase, and they were normalized using the normalization factor given by Serpent. The number of histories (source particles in Serpent and decays in Geant4) was 1 billion in the Sr-90 calculation and 100 million in the Y-90 case. Per-decay sampling was used with Geant4 version 10.4.

The calculated spectra are shown in Fig. 4.5 and 4.6. In both cases, the results agree reasonably well between about 0.12 and 0.3 MeV in Sr-90, and between 0.12 and 0.8 MeV in Y-90. Serpent overestimates the spectrum by about 2–5% at the peak region in both nuclides. Serpent clearly underestimates the spectrum at high energies in both cases. For example, the underestimation is 15-25% at 0.4 MeV in Sr-90, and at 1.5 MeV in Y-90. The underestimation is most likely caused by the limitations of the TTB approximation used in Serpent. The electron counts obtained with Geant4 were 0.35% and 2.7% of the photon counts on the tally surface in Sr-90 and Y-90, respectively. Thus, essentially all betas emitted by Sr-90 were stopped inside the pin, while some emitted by Y-90 escaped the pin. This means that the Geant4 spectrum for Y-90 would be slightly higher, if all the betas had stopped inside the pin.

A small peak can be seen at 1760 keV in the Y-90 spectrum calculated with Geant4. According to the LNHB data [37], this gamma peak corresponds to a $\beta^-_{0,1}$ transition which has a relative intensity of 0.0017 per decay. This gamma energy is not present in the ENDF/B-VII.1 decay data, which explains why it is not seen in the spectrum calculated with Serpent.

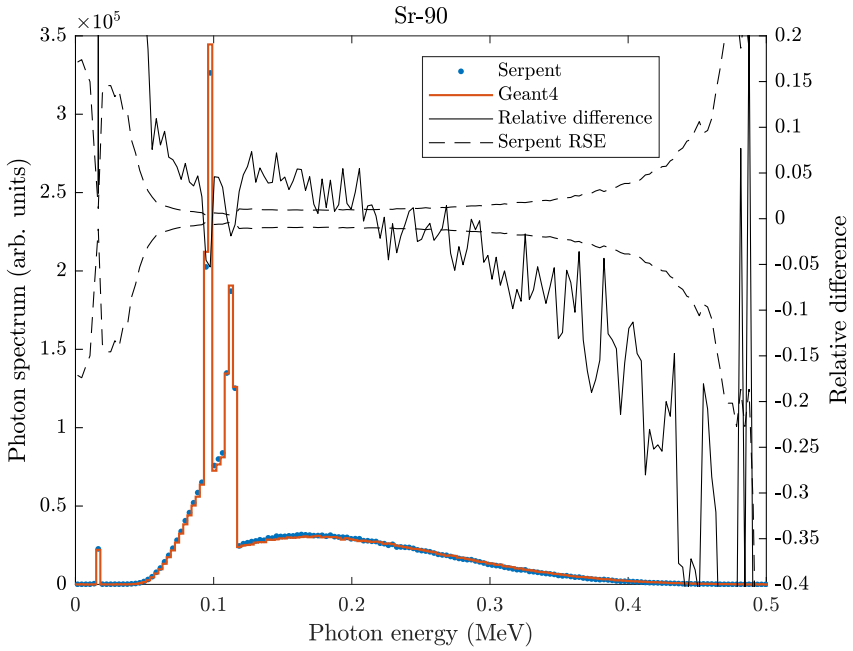

Figure 4.5: Photon spectrum at 1 cm from the fuel pin centre for Sr-90 calculated with Serpent and Geant4. Serpent RSE is the relative statistical error of the Serpent result.

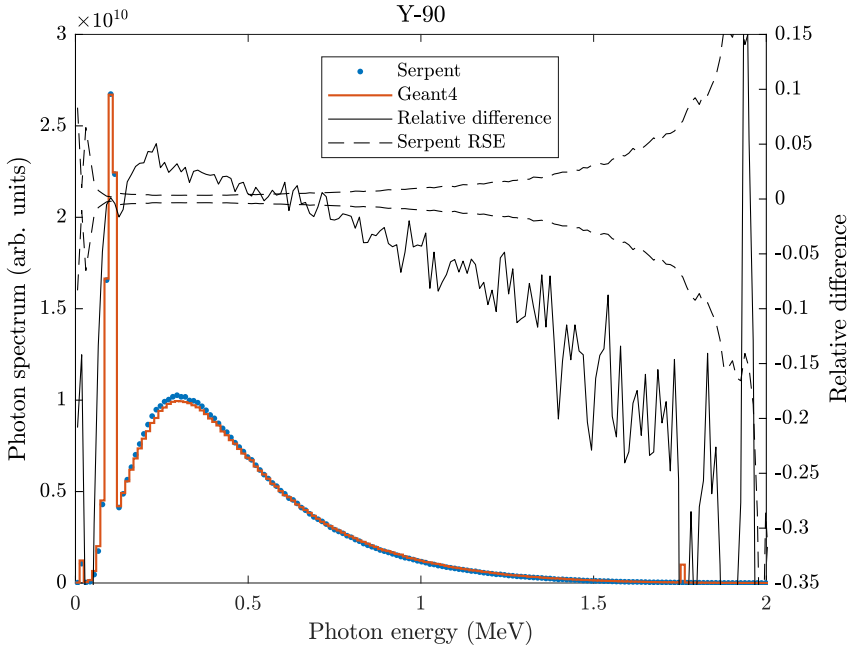

Figure 4.6: Photon spectrum at 1 cm from the fuel pin centre for Y-90 calculated with Serpent and Geant4. Serpent RSE is the relative statistical error of the Serpent result.

4.3 Comparison to RADAR beta spectrum data

In this test case, the beta decay model implemented in Serpent is studied by comparing it to the RADAR beta spectrum data [10] for a set of nuclides. The purpose of the test case is to study how much differences in beta spectrum affect effective

dose rate. The RADAR beta spectrum data is here considered more accurate than the spectra given by the Serpent model.

The fuel pin geometry used in the Geant4 comparison was also used in this test case, with the exception that the air cylinder around the fuel pin has a radius of 13 cm. Effective dose rate is calculated as a function of the distance from the pin in the air using the ICRP-116 antero-posterior flux-to-effective dose rate conversion factors [38]. The dose rates were calculated inside 1 cm × 1 cm × 100 cm volumes with a track-length detector.

The studied nuclides were Rb-82, Sr-89, Sr-90, Y-90, Cs-137 and Pr-144. Rb-82 is a strong β^+ emitter, which dominating decay branches are $\beta^+_{0,0}$ and $\beta^+_{0,1}$ with transition energies of 3381 keV and 2604 keV and relative intensities of 0.81 and 0.13 per decay, respectively. All the other nuclides are predominantly β^- emitters. Sr-89, Sr-90 and Y-90 can be regarded as pure β^- emitters. Cs-137 is also regarded here as a pure beta emitter because the 662 keV gamma emission from the metastable Ba-137m is treated separately in the ENDF/B-VII.1 decay data. In Pr-144, $\beta^-_{0,0}$ transition dominates with a relative intensity of 0.978.

The combined Sr-90/Y-90 and Cs-137/Ba-137m decays were also studied. The ratio of the atomic densities of two radioactive nuclides A and B, of which B has a shorter half-life and is formed by the decay of A, is in equilibrium given by

$$\frac{n_\mathrm{B}}{n_\mathrm{A}} = \frac{\lambda_\mathrm{A}}{\lambda_\mathrm{B} - \lambda_\mathrm{A}}, \tag{4.1}$$

where λ_A and λ_B are the half-lives of the nuclides. This ratio is about 1.61×10^{-7} for Ba-137m and Cs-137, and 2.54×10^{-4} for Y-90 and Sr-90. The used atomic densities were 4.82e-08 1/(barn cm) for Cs-137 and 7.34e-08 1/(barn cm) for Sr-90. In the case of Cs-137/Ba-137m, a calculation without the beta bremsstrahlung component was also done.

The beta spectra and calculated effective dose rates are shown for Rb-82, Sr-89 and Sr-90 in Fig. 4.7, and for Y-90, Cs-137 and Pr-144 in Fig. 4.8. In the case of Rb-82, there is an almost perfect match between the Serpent beta spectrum and RADAR data, and the effective dose rates are within statistical error. There are small differences in the Sr-89 spectrum, but the effective dose rates are nevertheless within statistical error. In the case of Sr-90, the RADAR spectrum is slightly higher at low energies, which results in 4–7% lower effective dose rates. This is also seen in Y-90 and Pr-144, for which the effective dose rate calculated with the RADAR data is about 2–3% lower. In Cs-137, the RADAR spectrum is also higher at low energies, but the effective dose rates are close to each other near the fuel pin. As the distance from the fuel pin increases, Serpent beta spectrum gives a higher dose rate.

The effective dose rates calculated for the Cs-137/Ba-137m decay is plotted in Fig. 4.9. The dose rates are all very close to each other. The contribution from the bremsstrahlung of Cs-137 is very small, only about 0.1–0.2%. Thus, beta bremsstrahlung is unimportant in Cs-137/Ba-137m decay, at least in this geometry. The dose rate for the Sr-90/Y-90 decay is presented in Fig. 4.10. The dose rate calculated

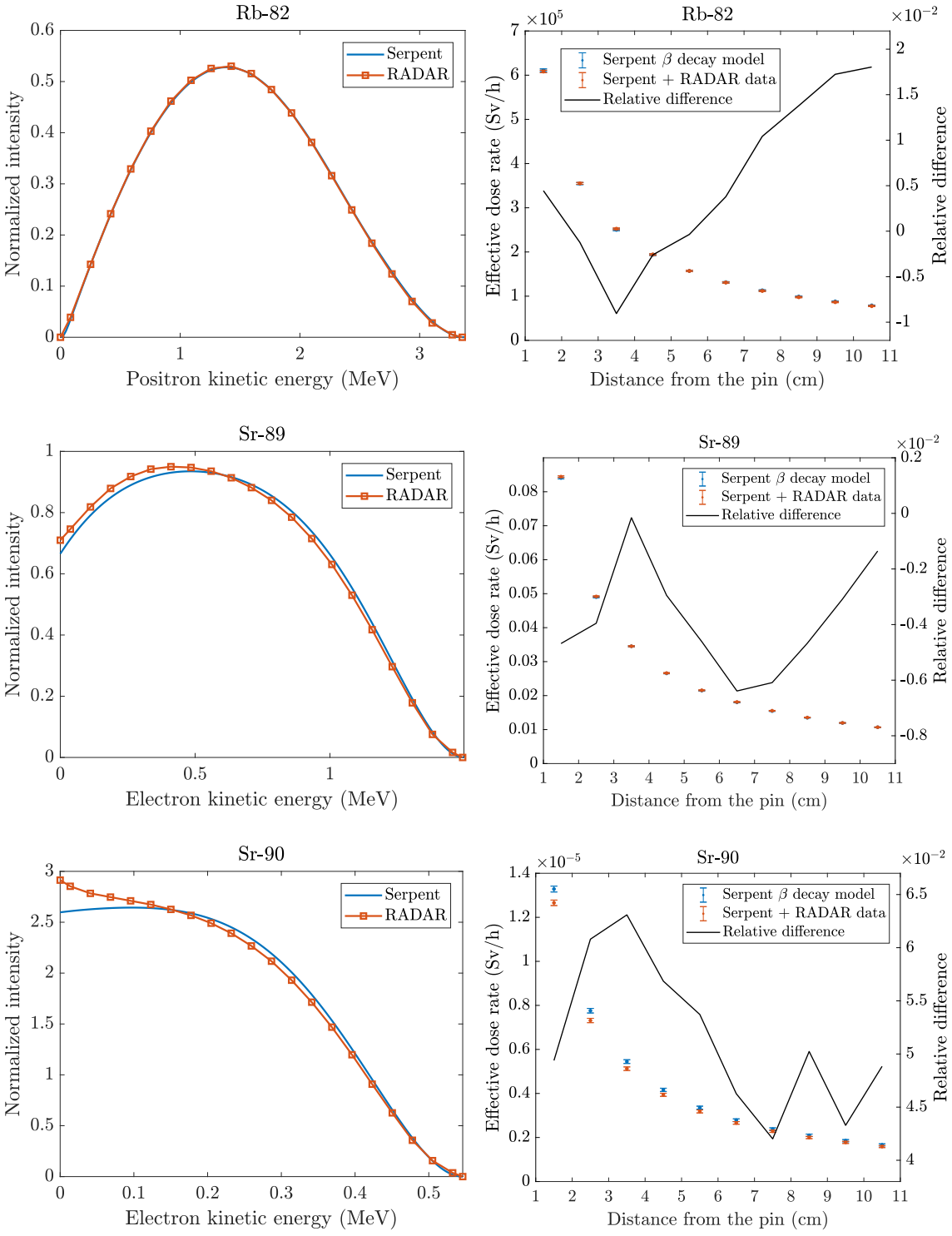

Figure 4.7: Left column: beta spectra according to the Serpent model and RADAR data. Right column: effective dose rates in the fuel pin test case calculated with the Serpent model and RADAR data and their relative difference.

with the RADAR data is about 2–3% lower, similar to the Y-90 case in Fig. 4.8. When compared to the effective dose rate from Sr-90 in Fig. 4.7 (the atomic density of Sr-90 was the same in both cases), it is seen that the contribution from Y-90 is much more important.

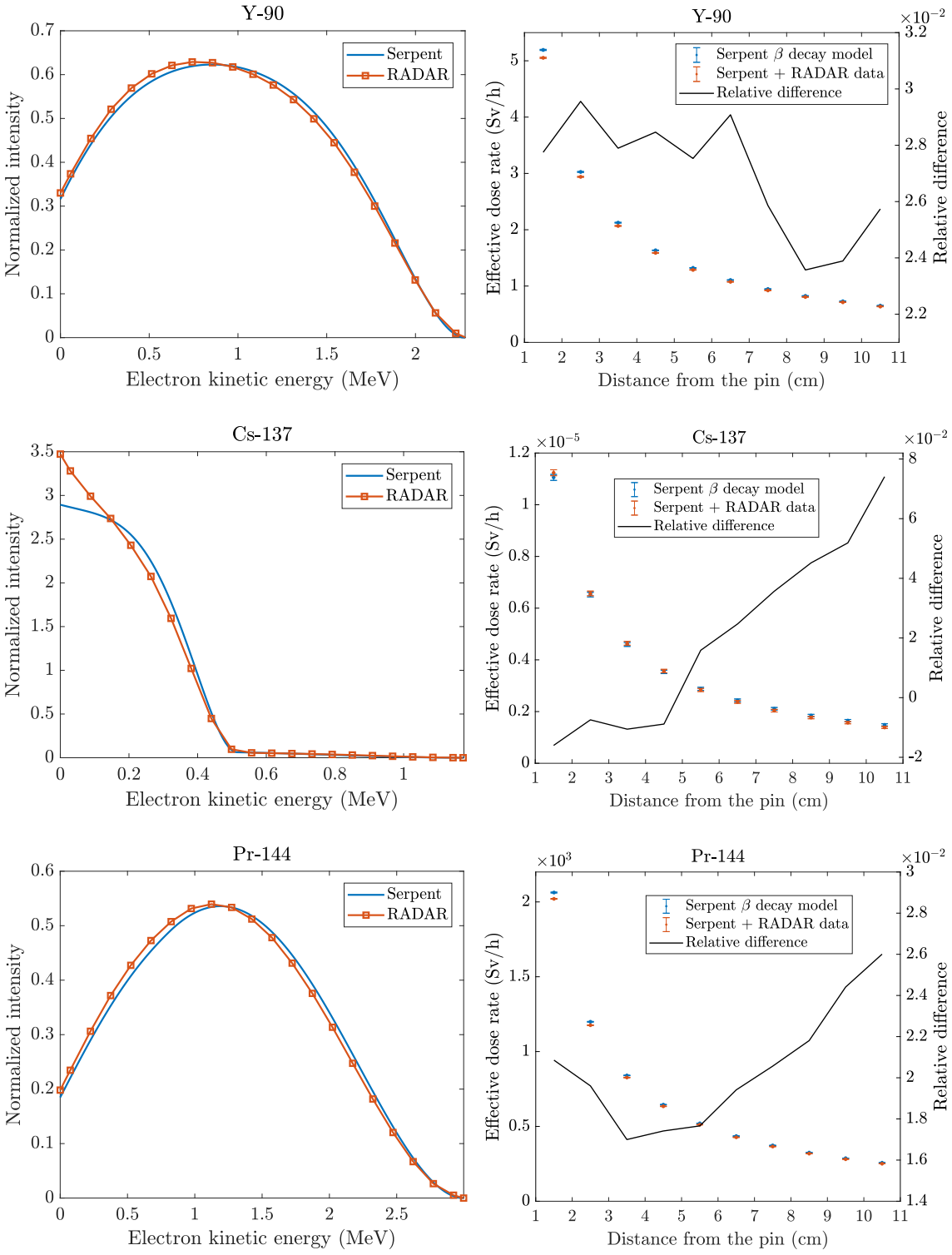

Figure 4.8: Left column: beta spectra according to the Serpent model and RADAR data. Right column: effective doses rate in the fuel pin test case calculated with the Serpent model and RADAR data and their relative difference.

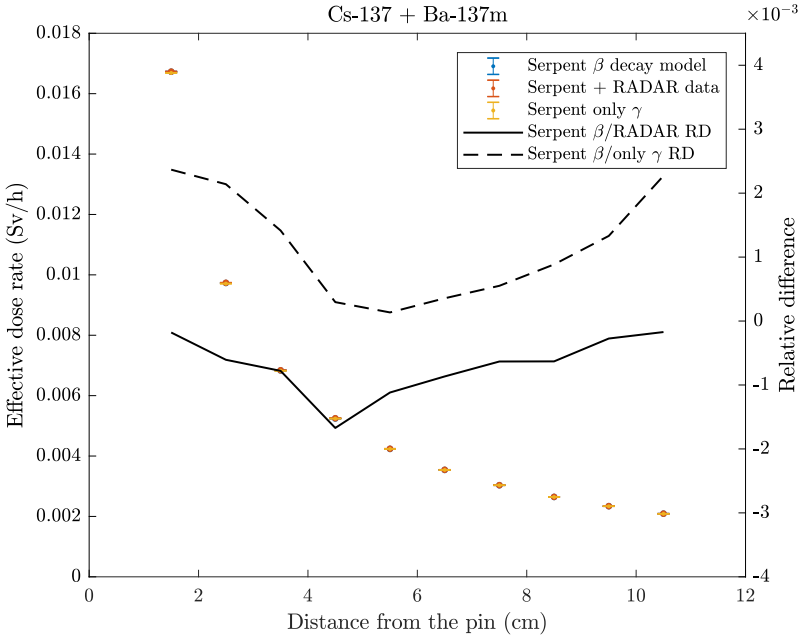

Figure 4.9: Effective doses rate in the fuel pin test case for the combined Cs-137 and Ba-137m decay calculated with the Serpent beta spectrum model, RADAR spectrum data, and without the beta bremsstrahlung component (only γ). Relative differences (RD) are also shown.

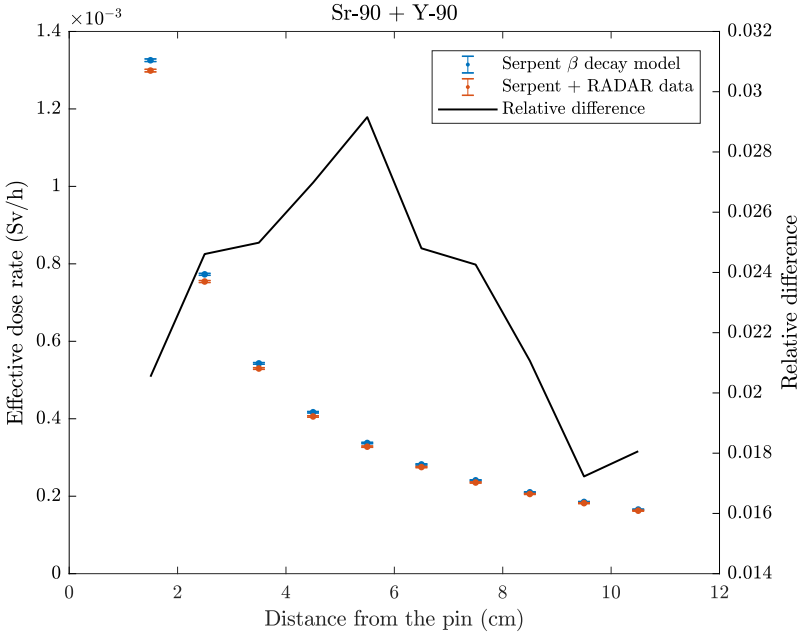

Figure 4.10: Effective doses rate in the fuel pin test case for Sr-90 and Y-90 decay calculated with the Serpent beta spectrum model and RADAR spectrum data.

5 Conclusions

A beta decay model was successfully implemented in Serpent. The new multiparticle decay source routine worked flawlessly in comparison to Serpent 2.1.29 and semi-analytically calculated spectrum. A reasonably good agreement with Geant4 was obtained in the peak region of bremsstrahlung spectrum for Sr-90 and Y-90. Serpent underestimated the high-energy regions of the spectra of several tens of percent, which is most likely caused by the limitations of the TTB approximation used for electrons and positrons in Serpent. In the case of a single fuel pin, the comparison with the RADAR beta spectrum data showed that 2–7% error can be expected in effective dose rate arising from beta bremsstrahlung. Although the Serpent beta decay model seemed to overestimate the effective dose rate in the tested nuclides, no general conclusions should be drawn from this because only a handful of nuclides were studied. It is important to note that the effective dose rate due to beta bremsstrahlung is estimated to be only about 10–20% of the total photon dose rate in spent fuel [6], which reduces the significance of the observed differences. Also, a single fuel pin can be considered to be a difficult test case. In a more complex geometry, for example in a fuel assembly, low-energy bremsstrahlung photons would experience stronger self-shielding than high-energy gammas.

The implemented beta decay model could be improved by introducing further corrections in the spectrum equation (2.6). In addition, the Fermi function approximation could be replaced with an accurate evaluation. One problem in improving the model is that the ENDF format decay data does not specify non-unique transitions separately. An alternative to improving the decay model would be to create a beta spectrum library with one of the beta spectrum codes listed in Sec. 2.2, e.g. with Radlist or BetaShape. However, none of these ideas are considered to be carried out in the near future, as the current beta decay model seems to work satisfactorily. More accurate beta spectra can be defined in the Serpent input file if needed by the user. Beta spectrum data included in the ICRP Publication 107 [27, 28] looks promising, and a support for its data format could be added in Serpent in the future.

The modified decay source routine is analog in the sense that the particle type is selected based on its emission rate in the material. If gammas are more important than the beta bremsstrahlung component, but the gamma emission rate is low compared to beta emission rate, calculation time is wasted in simulating the bremsstrahlung photons. To speed up the calculation, the emission probabilities of particle types could be user-defined parameters, in which case the weight of the emitted particles should be adjusted accordingly. In addition, energy-biasing for bremsstrahlung could be implemented. Most bremsstrahlung photons have low energies and are thus absorbed in short distances in heavy materials, resulting in waste of computation time.

The applicability of the implemented beta decay model for decay heat calculations was not studied. Currently, the total decay heat in Serpent is given by the sum of the average energy of light particles (betas, conversion electrons, etc.), electromagnetic radiation (gamma-rays, fluorescence, annihilation photons, etc.) and heavy particles (recoil energies, neutrons, etc.). This decay heat is assumed to be deposited at the

decay location. To estimate the spatial distribution of decay heat more precisely, it should consist of the locally deposited part, which is formed by the average energy of heavy particles and the portion of beta particle energy that is not emitted as bremsstrahlung, and the transported part, which is calculated for the electromagnetic radiation components and beta bremsstrahlung. If decay heat calculations that take into account bremsstrahlung from beta decay are to be performed in the future, the accuracy of the average beta energies calculated with the Serpent beta decay model should be studied first.

References

[1] A. Nichols, "Summary Report of Consultants' Meeting on Beta-Decay and Decay Heat, Vienna, 12-14 December 2005," International Atomic Energy Agency, Vienna, Austria (2006).

[2] J. S. Welsh, "Beta decay in science and medicine.," *American journal of clinical oncology*, **30**, *4*, 437–439 (2007).

[3] M. Bardies and J.-F. Chatal, "Absorbed doses for internal radiotherapy from 22 beta-emitting radionuclides: beta dosimetry of small spheres," *Physics in Medicine & Biology*, **39**, *6*, 961 (1994).

[4] M. A. Prelas et al., "A review of nuclear batteries," *Progress in Nuclear Energy*, **75**, 117–148 (2014).

[5] L. Jødal, "Beta emitters and radiation protection," *Acta Oncologica*, **48**, *2*, 308–313 (2009).

[6] O. Hermann and C. Alexander, "Review of spent-fuel photon and neutron source spectra," Oak Ridge National Lab., TN (USA) (1986).

[7] J. Leppänen, M. Pusa, T. Viitanen, V. Valtavirta, and T. Kaltiaisenaho, "The Serpent Monte Carlo code: Status, development and applications in 2013," *Annals of Nuclear Energy*, **82**, 142–150 (2015).

[8] T. Kaltiaisenaho, "Implementing a photon physics model in Serpent 2," Master's thesis, Aalto University, 2016.

[9] J. Allison et al., "Recent developments in Geant4," *Nuclear Instruments and Methods in Physics Research Section A: Accelerators, Spectrometers, Detectors and Associated Equipment*, **835**, 186–225 (2016).

[10] "RADAR - The Decay Data," RADAR - the RAdiation Dose Assessment Resource, `http://www.doseinfo-radar.com`, [accessed: 20 January 2018].

[11] E. Podgorsak, *Radiation Physics for Medical Physicists*, Biological and Medical Physics, Biomedical Engineering, Springer-Verlag Berlin Heidelberg (2010).

[12] X. Mougeot, "Reliability of usual assumptions in the calculation of β and ν spectra," *Phys. Rev. C*, **91**, 055504 (2015).

[13] Mougeot, Xavier, "BetaShape: A new code for improved analytical calculations of beta spectra," *EPJ Web Conf.*, **146**, 12015 (2017).

[14] E. J. Konopinski, *The Theory of Beta Radioactivity*, Oxford University Press (1966).

[15] G. Schenter and P. Vogel, "A simple approximation of the Fermi function in nuclear beta decay," *Nuclear Science and Engineering*, **83**, *3*, 393–396 (1983).

[16] P. Venkataramaiah, K. Gopala, A. Basavaraju, S. S. Suryanarayana, and H. Sanjeeviah, "A simple relation for the Fermi function," *Journal of Physics G: Nuclear Physics*, **11**, *3*, 359 (1985).

[17] M. Rose, "Beta-and Gamma-Ray Spectroscopy," *JS'oith-Holland Publishing Co* (1955).

[18] M. Chadwick et al., "ENDF/B-VII.1 Nuclear Data for Science and Technology: Cross Sections, Covariances, Fission Product Yields and Decay Data," *Nuclear Data Sheets*, **112**, *12*, 2887–2996 (2011).

[19] M. Kellett, O. Bersillon, and R. W. Mills, *JEFF Report 20: The JEFF-3.1/-3.1.1 radioactive decay data and fission yields sub-libraries* (2009).

[20] M. A. Kellett and O. Bersillon, "The Decay Data Evaluation Project (DDEP) and the JEFF-3.3 radioactive decay data library: Combining international collaborative efforts on evaluated decay data," *Proc. EPJ Web of Conferences*, volume 146, p. 02009, EDP Sciences, 2017.

[21] J. Katakura and M. F, "JENDL Decay Data File 2015," JAEA-Data/Code 2015-030 (2016).

[22] M. Herman et al., "ENDF-6 Formats Manual Data Formats and Procedures for the Evaluated Nuclear Data File ENDF/B-VI and ENDF/B-VII," Brookhaven National Laboratory (BNL) National Nuclear Data Center (2009).

[23] J. Katakura, "JENDL FP Decay Data File 2011 and Fission Yields Data File 2011," JAEA-Data/Code 2011-025 (2012).

[24] M. Stabin et al., "RADAR: the radiation dose assessment resource—an online source of dose information for nuclear medicine and occupational radiation safety," *J Nucl Med*, **42**, *5*, 243P (2001).

[25] K. Eckerman, R. Westfall, J. Ryman, and M. Cristy, "Availability of nuclear decay data in electronic form, including beta spectra not previously published," *Health physics*, **67**, *4*, 338–345 (1994).

[26] T. W. Burrows, "The program RADLST (Radiation Listing)," Brookhaven National Lab., Upton, NY (USA) (1988).

[27] K. Eckerman and A. Endo, "ICRP Publication 107. Nuclear decay data for dosimetric calculations.," *Annals of the ICRP*, **38**, *3*, 7–96 (2008).

[28] "ICRP CD1 - Nuclear Decay Data for Dosimetric Calculations, Supplemental Material," Annals of the ICRP, `http://journals.sagepub.com/doi/suppl/10.1177/ANIB_38_3`, [accessed: 22 February 2018].

[29] A. Tobias, G. Panini, and F. Leszczynski, "BTPLOT BTSPEC EXSPEC ORDTAB TABLST, Retrieval of ENDF/B Decay Spectra," (2002).

[30] J. Dickens, "Electron spectra from decay of fission products," ORNL/TM-8285, Oak Ridge National Lab., TN (USA) (1982).

[31] "NEA-0866 BTPLOT, BTSPEC, EXSP," NEA Data Bank, http://www.oecd-nea.org/tools/abstract/detail/nea-0866, [accessed: 13 January 2018].

[32] "DLC-0100 ZZ-ELECSPEC," NEA Data Bank, http://www.oecd-nea.org/tools/abstract/detail/dlc-0100/, [accessed: 13 January 2018].

[33] "ENSDF Analysis and Utility Programs," IAEA Nuclear Data Services, https://www-nds.iaea.org/public/ensdf_pgm/, [accessed: 13 January 2018].

[34] M. Xavier, "BetaShape - Calculs de spectres bêta / Beta spectra calculations, Version: 1.0 (24/06/2016)," Laboratoire National Henri Becquerel, http://www.nucleide.org/logiciels.htm, [accessed: 13 January 2018].

[35] N. Soppera, M. Bossant, and E. Dupont, "JANIS 4: An improved version of the NEA java-based nuclear data information system," *Nuclear Data Sheets*, **120**, 294–296 (2014).

[36] S. Hauf et al., "Radioactive decays in Geant4," *IEEE Transactions on Nuclear Science*, **60**, *4*, 2966–2983 (2013).

[37] "Atomic and Nuclear data," Laboratoire National Henri Becquerel, http://www.lnhb.fr/nuclear-data/, [accessed: 20 January 2018].

[38] N. Petoussi-Henss et al., "Conversion Coefficients for Radiological Protection Quantities for External Radiation Exposures," *Annals of the ICRP*, **40**, *2-5*, 1–257 (2010).